DOI: 10.6060/mhc256900b

Unexpected Reactivity of 2,3-Diaminoporphyrins with β-Diketones

Ekaterina S. Shremzer,[a] Kirill P. Birin,[a@] and Aslan Yu. Tsivadze[a,b]

[a]*Frumkin Institute of Physical Chemistry and Electrochemistry Russian Academy of Sciences, 119071 Moscow, Russia*
[b]*Kurnakov Institute of General and Inorganic Chemistry Russian Academy of Sciences, 119991 Moscow, Russia*
[@]*Corresponding author E-mail: kirill.birin@gmail.com*

The condensation of 2,3-diaminoporphyrins with various 1,3-diketones was investigated to reveal the key structural and electronic factors determining the formation of heterocycle-appended porphyrins. The reaction of an unsubstituted β-diketone with diaminoporphyrin led to fusion with a seven-membered diazepine ring, accompanied by oxidative degradation of the heterocycle and formation of N-acylated derivative. However, sterically hindered β-diketones and α,α-disubstituted derivatives effectively suppressed these side reactions, favoring the selective formation of stable pyrazine-appended porphyrins. The observed reactivity trends emphasize the role of steric effects, the position of substituents, and thermodynamic stability in directing the condensation pathway. UV-Vis analysis of the resulting pyrazinoporphyrins revealed significant bathochromic shifts in both the Soret and Q-bands, confirming expanded π-conjugation.

Keywords: Heterocycle-appended porphyrins, 2,3-diaminoporphyrin, condensation, diazepines, 1,3-diketones.

Необычная реакционная способность 2,3-диаминопорфиринов в конденсации с β-дикетонами

Е. С. Шремзер,[a] К. П. Бирин,[a@] А. Ю. Цивадзе[a,b]

[a]*Федеральное государственное бюджетное учреждение науки Институт физической химии и электрохимии им. А.Н. Фрумкина Российской академии наук, 119071 Москва, Россия*
[b]*Федеральное государственное бюджетное учреждение науки Институт общей и неорганической химии им. Н.С. Курнакова Российской академии наук, 119991 Москва, Россия*
[@]*E-mail: kirill.birin@gmail.com*

В настоящей работе изучено взаимодействие 2,3-диаминопорфиринов с различными 1,3-дикетонами, что позволило выявить ключевые структурные факторы, определяющие образование гетероцикл-аннелированных порфиринов различной природы. Взаимодействие незамещённого β-дикетона с диаминопорфирином приводила к образованию семичленного диазепинового цикла на периферии порфирина, а также к образованию N-ацилированного производного вследствие окислительной деградации диазепинового фрагмента. В то же время взаимодействие диаминопорфирина со стерически нагруженными β-дикетонами и α,α-дизамещёнными производными приводило к селективному образованию пиразинопорфиринов. Выявленные тенденции реакционной способности подчёркивают определяющую роль стерических факторов, природы заместителей и термодинамической устойчивости для определения пути протекания конденсации. В электронных спектрах поглощения полученных пиразинопорфиринов наблюдались батохромные сдвиги как Soret-полос, так и Q-полос, что свидетельствует о расширении π-системы.

Ключевые слова: Гетероцикл-аннелированные порфирины, 2,3-диаминопорфирин, реакция конденсации, диазепины, 1,3-дикетоны.

Introduction

Porphyrins are widely recognized as versatile macrocyclic compounds with broad applicability in catalysis,[1–5] medicine,[6] photodynamic therapy,[7,8] and materials science.[9–11] Their broad adaptability stems from the ability to fine-tune their photophysical and electrochemical properties through targeted functionalization of the tetrapyrrolic macrocycle.[12] Functionalization strategies primarily involve modifications of the pyrrolic subunits[13,14] or the introduction of functional groups on the macrocycle periphery,[15,13] facilitating the development of advanced materials tailored to specific applications.

Among various functionalization approaches, the incorporation of N-heterocyclic fragments into porphyrin frameworks has garnered significant attention and offers a powerful means to fine-tune their electronic, photophysical, and catalytic properties.[15-18] The presence of a heteroatom can markedly influence electronic delocalization and modify the conjugation of porphyrins.[13] N-Heterocycles are ubiquitous in biologically active and pharmaceutically relevant compounds, playing essential structural and functional roles.[19,20] For instance, benzimidazole fragments[21] are commonly utilized in drug design, while pyridine-based heterocycles[16] play critical roles in vitamins, alkaloids, and cofactors. Additionally, N-heterocyclic carbenes have emerged as potent catalytic moieties.[22] Among these, seven-membered heterocycles such as diazepines represent a privileged scaffold in medicinal chemistry due to their diverse biological activities and structural flexibility.[23,24] These structures are prevalent in a broad spectrum of biologically active molecules, including pharmaceuticals used as anxiolytics, sedatives, anticonvulsants, and muscle relaxants.[25] The dynamic enamine/diimine tautomerism, tuneable acid-base behaviour, hydrogen bonding capability, and inherent conformational flexibility collectively define their unique properties.[26] Given the exceptional properties and broad functionality of diazepine derivatives, along with the photophysical characteristics of the porphyrin core, the integration of these heterocyclic units within a single molecule presents compelling opportunities to expand the functional scope of porphyrin-based hybrid systems, which can lead to manifold applications (electrical conductivity, nonlinear optical properties, photocatalysis, *etc*.). In this context, the development of efficient synthetic methodologies for diazepine-functionalized porphyrins remains a critical challenge.

The incorporation of fused diazepine motifs into porphyrins remains largely underdeveloped. In contrast, structurally related tetrapyrrolic systems such as porphyrazines have seen substantial progress in this direction, demonstrating the value of such modification.[27–38] For instance, diazepino-porphyrazines exhibit distinct characteristics, including non-planarity, enhanced Stokes' shifts, tautomeric flexibility, and strong aggregation tendencies driven by intermolecular hydrogen bonding. Their electronic absorption spectra differ from those of phthalocyanines, displaying additional transitions in the Q-band region, while their fluorescence properties can be tuned by solvent polarity and peripheral substituents. These compounds are typically synthesized *via* template-based cyclotetramerization of dinitrile precursors featuring 1,4-diazepine fragments.[37,38]

A critical distinction in the synthesis of *β,β'*-appended porphyrins lies in their post-synthetic modification, as total synthesis *via* condensation of *β,β'*-fused pyrrole or dipyrromethane derivatives is often impeded by low yields and constitutional isomer formation.[13] Previous studies have demonstrated the reactivity of 2,3-diaminoporphyrins, establishing them as valuable precursors for heterocycle-appended porphyrins through condensation with aromatic carbonyl compounds, leading to the formation of imidazole- and pyrazine-appended porphyrins.[4,39–42] In turn, the synthesis of diazepines has been extensively explored, with numerous methodologies developed to efficiently construct the diazepine core.[43–46] One of the most common synthetic strategies involves the condensation of *o*-phenylenediamines or similar 1,2-diamines with 1,3-diketones[47–50,44] or other carbonyl-containing compounds,[51] such as chalcone derivatives.[52,53]

Building on these findings, we propose that 2,3-diaminoporphyrin can serve as an effective diamine precursor for the synthesis of diazepine-appended porphyrins. The use of 1,3-diketones as the ketone component enables a condensation reaction, facilitating the formation of fused porphyrin-diazepine frameworks.

In light of these considerations, this study explores new pathways for the functionalization of porphyrins with heterocyclic diazepine units by investigating the reactivity of 2,3-diaminoporphyrins with *β*-diketones. By addressing key synthetic challenges, this work aims to expand the structural and functional diversity of porphyrin derivatives, thereby contributing to the broader goal of developing innovative materials for interdisciplinary applications.

Experimental

Materials and methods

All the used reagent grade chemicals were purchased from commercial suppliers, unless otherwise noted. The solvents have been purified according to conventional methods.[54]

Chromatographic purification was performed at Machery-Nagel Silica 60 (0.063–0.2 mm). Merck aluminum plates (TLC Silica 60 F254) were used for TLC analysis which was performed with dichloromethane as an eluent.

NMR spectra were recorded on Avance III spectrometer (Bruker) with a proton frequency of 600.13 MHz in $CDCl_3$ at *ca*. 10^{-4} M at 303 K using the resonance of the residual $CHCl_3$ (δ = 7.26 ppm) as an internal reference. Variable-temperature experiments were performed with ±0.1 K accuracy. Complete NMR spectra of obtained compounds are summarized in *Supplementary Materials*.

MALDI-TOF mass-spectra were recorded using a Ultraflex spectrometer (Bruker Daltonics) in positive ions mode without matrix. An Agilent 1260 chromatographic system (Agilent, USA) equipped with Bruker Maxis Impact quadrupole and time-of-flight mass spectrometric detector (Bruker, Germany) was used to record high-resolution mass-spectra (HRMS). Complete profiles of mass-spectra of compounds are presented in *Supplementary Materials.*

UV-Vis spectra were recorded on Evolution 220 spectrophotometer (Thermo Scientific) in the 250–900 nm range in rectangular quartz cells with optical paths of 10 mm.

Synthesis

General procedure of condensation reaction with β-diketones. A two-necked round-bottomed flask was charged with **Ni-1** (0.05 mmol) and repeatedly purged with argon. Under an inert atmosphere, freshly distilled dichloromethane (DCM, 16 mL), 10% Pd/C (50 mg), $NaBH_4$ (29 mg, 0.75 mmol), and freshly

distilled methanol (MeOH, 0.6 mL) were added sequentially. The reaction mixture was stirred at room temperature until complete reduction was confirmed by TLC (SiO_2, DCM). The Pd/C catalyst was then removed by filtration through a Celite-545 pad. To the resulting solution containing **Ni-2**, 1,3-diketone (1.2–50 mmol depending on substrate) was added, and the mixture was stirred under air at ambient temperature for 24–48 h. The solvent was then evaporated to dryness; the crude product was purified by chromatography over silica.

*Mixture of **Ni-3** and **Ni-4*** was obtained from **Ni-1** (58 mg, 0.057 mmol) and acetyleacetone (0.58 mL, 5.7 mmol, 100 eq.). The residue, purified by chromatography over silica using mixtures of dichloromethane/methanol (100:0 to 97:3, v/v), afforded 38 mg of a mixture of compounds in a 1:1 ratio, as determined by ^{1}H NMR. The yields of **Ni-3** and **Ni-4** were both 32%. ^{1}H NMR (600 MHz, $CDCl_3$) δ_H ppm (*J*, Hz): 8.76 (d, ^3J = 4.9, 2H, $H_{\beta\ -\ Ni\text{-}3}$), 8.73 – 8.70 (m, 4H, $H_{\beta\ -\ Ni\text{-}3}$), 8.70–8.66 (m, 4H, $H_{\beta\ -\ Ni\text{-}4}$), 8.60 (d, ^3J = 5.0, 1H, $H_{\beta\ -\ Ni\text{-}4}$), 8.56 (d, ^3J = 4.9, 1H, $H_{\beta\ -\ Ni\text{-}4}$), 7.91 (d, ^3J = 8.1, 4H, $H_{o\ -\ Ni\text{-}3}$), 7.88 (d, ^3J = 8.2, 4H, $H_{o\ -\ Ni\text{-}4}$), 7.84 (d, ^3J = 8.2, 2H, $H_{o\ -\ Ni\text{-}4}$), 7.80 (d, ^3J = 8.2, 2H, $H_{o\ -\ Ni\text{-}4}$), 7.66 (br s, 4H, $H_{o\ -\ Ni\text{-}3}$), 7.24 – 7.17 (m, 12H, $H_{m\ -\ both}$), 7.12 (d, *J* = 8.1, 4H, $H_{m\ -\ Ni\text{-}3}$), 6.99 (s, 1H, $NHAc_{\ -\ Ni\text{-}4}$), 4.64 (s, 2H, $NH_{2\ -\ Ni\text{-}4}$), 4.24 – 4.11 (m, 16H, $O\text{-}CH_{2\ -\ both}$), 2.04 (s, 6H, $Methyl_{\ -\ Ni\text{-}3}$), 1.99 – 1.87 (m, 16H, $CH_{2\ -\ both}$), 1.81 (s, 3H, $Methyl_{\ -\ Ni\text{-}4}$), 1.68 – 1.58 (m, 16H, $CH_{2\ -\ both}$), 1.13–1.01 (m, 24H, $CH_{3\ -\ both}$). ^{13}C NMR (151 MHz, $CDCl_3$) δ_C ppm: 166.99, 159.72, 159.39, 159.15, 159.11, 158.76, 146.34, 146.16, 144.23, 144.06, 143.64, 143.04, 142.63, 142.33, 142.13, 142.08, 142.05, 141.50, 136.64, 135.75, 134.88, 134.86, 134.80, 134.44, 133.61, 133.59, 133.18, 133.03, 133.01, 133.00, 132.64, 132.10, 131.90, 131.74, 131.68, 131.58, 131.55, 131.40, 131.25, 131.23, 130.85, 120.11, 119.32, 118.88, 118.02, 116.92, 116.14, 114.35, 114.06, 113.11, 112.90, 68.26, 68.17, 68.14, 68.11, 45.77, 31.67, 31.66, 31.58, 31.51, 26.72, 23.36, 19.55, 19.52, 19.51, 19.46, 14.10, 14.08, 14.06, 14.00. MS (MALDI TOF) *m/z*: $[M]^+$ calcd. for $C_{62}H_{62}N_6NiO_5$ (for ^{58}Ni) 1030.43, found 1030.29; *m/z* $[M]^+$ calcd. for $C_{65}H_{66}N_6NiO_4$ (for ^{58}Ni) 1052.45, found 1052.31.

Ni-5 was synthesized from **Ni-1** (38 mg, 0.037 mmol) and 1,3-diphenylpropane-1,3-dione (314 mg, 1.4 mmol, 38 eq.). The residue, purified by chromatography over silica using mixtures of hexane/dichloromethane (4:1 to 7:3, v/v), afforded 20 mg of **Ni-5** in 50% yield. ^{1}H NMR (600 MHz, $CDCl_3$) δ_H ppm (*J*, Hz): 9.26 (s, 1H, H_{Pz}), 8.86 (d, ^3J = 4.9, 1H, Hβ), 8.76–8.69 (m, 5H, Hβ), 8.00–7.95 (m, 2H, H_m-C_6H_5), 7.89 (d, ^3J = 8.4, 4H, H_o), 7.84 (d, ^3J = 8.4, 2H, H_o), 7.79 (d, ^3J = 8.4, 2H, H_o), 7.48–7.43 (m, 3H, H_o-C_6H_5 and H_p-C_6H_5), 7.26–7.23 (m, 2H, H_m), 7.23–7.18 (m, 6H, H_m), 4.28–4.22 (m, 4H, O-CH_2), 4.20 (t, ^3J = 6.5, 4H, O-CH_2), 2.04–1.98 (m, 2H, CH_2), 1.97–1.90 (m, 6H, CH_2), 1.75–1.67 (m, 2H, CH_2), 1.67–1.59 (m, 6H, CH_2), 1.15–1.04 (m, 12H, CH_3). ^{13}C NMR (151 MHz, $CDCl_3$) δ_C ppm: 159.36, 159.27, 159.12 ($C_{Ar'}$); 149.74, 148.96 (C_β); 148.41 (C_{Pz}); 144.45, 144.19, 142.73, 142.67, 141.91, 141.89 (C_α); 139.57 (CH_{Pz}); 137.27 (C_{Ph}); 134.78, 134.33, 134.15 (CH_o); 133.18, 133.07 (C_α); 132.91 (CH_β and C_{Ar}); 132.86 (CH_β); 132.64, 132.61 (C_{Ar}); 132.06, 132.02, 131.93, 131.77 (CH_β); 129.80 ($CH_{p\text{-}Ph}$); 128.85 ($CH_{o\text{-}Ph}$); 127.57 ($CH_{m\text{-}Ph}$); 120.38, 120.31, 116.53, 116.48 (C_{meso}); 113.29, 113.24, 113.15 (CH_m); 68.14, 68.10, 68.03 (O-CH_2); 31.92, 31.78, 31.66 (CH_2); 19.69, 19.61, 19.55 (CH_2); 14.18, 14.16, 14.10 (CH_3). HRMS ESI *m/z*: $[M+H]^+$ calcd. for $C_{68}H_{65}N_6NiO_4$ (for ^{58}Ni) 1087.4421, found 1087.4539. UV-Vis ($CHCl_3$) λ_{max} nm (lg ε): 335 (4.51), 440 (5.31), 549 (4.27), 581 (3.91).

Ni-6 was synthesized from **Ni-1** (30 mg, 0.03 mmol) and 1,3-bis(4-(*tert*-butyl)phenyl)propane-1,3-dione (152 mg, 0.45 mmol, 15 eq.). The residue, purified by chromatography over silica using mixtures of hexane/dichloromethane (4:1 to 3:2, v/v), afforded 34 mg of **Ni-6** in 41% yield. ^{1}H NMR (600 MHz, $CDCl_3$) δ_H ppm (*J*, Hz): 9.24 (s, 1H, H_{Pz}), 8.87 (d, ^3J = 4.9, 1H, Hβ), 8.76–8.70 (m, 5H, Hβ), 7.92 (d, ^3J = 8.3, 2H, H_m-^{t}*Bu*-C_6H_4), 7.89 (d, ^3J = 8.3, 4H, H_o), 7.84 (d, ^3J = 8.4, 2H, H_o), 7.79 (d, ^3J = 8.4, 2H, H_o), 7.49 (d, ^3J = 8.4, 2H, H_o-^{t}*Bu*-C_6H_4), 7.27 (d, ^3J = 8.5, 2H, H_m), 7.24–7.18 (m, 6H, H_m), 4.26–4.18 (m, 8H, O-CH_2), 1.99–1.90 (m, 8H, CH_2), 1.69–1.59 (m, 8H, CH_2), 1.41 (s, 9H, CH_3-^{t}*Bu*), 1.11–1.05 (m, 12H, CH_3). ^{13}C NMR (151 MHz, $CDCl_3$) δ_C ppm: 159.33, 159.26, 159.10 ($C_{Ar'}$); 153.13($C_{Ph'}$); 149.84, 148.76 (C_β); 148.41 (C_{Pz}); 144.45, 144.15, 142.68, 142.61, 141.84, 141.83 (C_α); 139.46 (CH_{Pz}); 134.77 (CH_o); 134.44 (C_{Ph}); 134.33, 134.14 (CH_o); 133.28, 133.13 (C_α); 132.95 (C_{Ar}); 132.89, 132.84 (CH_β); 132.66 (C_{Ar}); 132.02, 131.97, 131.91, 131.72 (CH_β); 127.30 (CH_m-^{t}*Bu*-C_6H_4); 125.83 (CH_o-^{t}*Bu*-C_6H_4); 120.35, 120.26, 116.50, 116.36 (C_{meso}); 113.26, 113.23, 113.14 (CH_m); 68.19, 68.13, 68.03 (O-CH_2); 34.94 ($C_{\text{-}t\text{Bu}}$); 32.04, 31.78, 31.66 (CH_2); 31.41 ($CH_{3\text{-}t\text{Bu}}$); 19.87, 19.60, 19.55 (CH_2); 14.22, 14.16, 14.10 (CH_3). HRMS ESI *m/z*: $[M+H]^+$ calcd. for $C_{72}H_{73}N_6NiO_4$ (for ^{58}Ni) 1143.5047, found 1143.5109. UV-Vis ($CHCl_3$) λ_{max} nm (lg ε): 337 (4.43), 440 (5.20), 547 (4.20), 582 (3.88).

Ni-7 was synthesized from **Ni-1** (66 mg, 0.065 mmol) and 3,3-dimethyl-2,4-pentanedione (0.22 mL, 1.7 mmol, 24 eq.). The residue, purified by chromatography over silica over silica using mixtures of hexane/dichloromethane (4:1 to 3:2, v/v), afforded 41 mg of **Ni-7** in 60% yield. ^{1}H NMR (600 MHz, $CDCl_3$) δ_H ppm (*J*, Hz): 8.82 (d, ^3J = 4.9, 2H, Hβ), 8.75 (d, ^3J = 4.9, 2H, Hβ), 8.73 (s, 2H, Hβ), 7.90 (d, *J* = 8.4, 4H, H_o), 7.76 (d, ^3J = 8.4, 4H, H_o), 7.22–7.17 (m, 8H, H_m), 4.26–4.18 (m, 8H, O-CH_2), 2.55 (s, 6H, Methyl), 2.00–1.90 (m, 8H, CH_2), 1.69–1.60 (m, 8H, CH_2), 1.13–1.06 (m, 12H, CH_3). ^{13}C NMR (151 MHz, $CDCl_3$) δ_C ppm: 159.20, 159.10 ($C_{Ar'}$); 150.30 (C_{Pz}); 148.36 (C_β); 144.17, 142.47, 141.66 (C_α); 134.77, 134.25 (CH_o); 133.58 (C_α); 132.93, 132.81 (C_{Ar}); 132.66, 131.82, 131.65 (CH_β); 120.04, 116.24 (C_{meso}); 113.18, 113.06 (CH_m); 68.19, 68.11 (O-CH_2); 31.66 (CH_2); 23.45 (Methyl); 19.54 (CH_2); 14.09 (CH_3). MS (MALDI TOF) *m/z*: $[M]^+$ calcd for $C_{64}H_{64}N_6NiO_4$ (for ^{58}Ni) 1038.43, found 1038.08. UV-Vis ($CHCl_3$) λ_{max} nm (lg ε): 311 (4.42), 431 (5.37), 541 (4.21), 577 (3.88).

Results and Discussion

2,3-Diaminoporphyrins represent a versatile synthetic platform owing to their high reactivity, which enables condensation with aromatic aldehydes and polycyclic aromatic diketones to yield five- or six-membered heterocycle-appended porphyrins. A typical synthetic route involves the preparation of 2-amino-3-nitroporphyrin, followed by its reduction to 2,3-diaminoporphyrin using 10% Pd/C in a dichloromethane/methanol mixture. The resulting diamine then undergoes condensation with various carbonyl-containing compounds. In an effort to synthesize a porphyrin bearing a seven-membered heterocyclic fragment on its periphery, we adopted a similar strategy, employing *β*-diketones as dicarbonyl precursors.

2-Nitro-3-amino-tetra(4-butoxyphenyl)porphyrinate of nickel(II) **Ni-1** was employed as the starting material. The combination of 4-butoxyphenyl *meso*-substituents and the coordination of nickel(II) provides synergistic effect, making the tetrapyrrolic framework especially favourable for heterocyclic annelation.[55,40] The long alkyl chains of the 4-butoxyphenyl groups enhance solubility in organic media,[40] while nickel(II) coordination, which suppresses fluorescence, plays a pivotal role in stabilizing the diaminoporphyrin intermediate, preventing oxidative degradation and facilitating a more controlled condensation process. Moreover, the diamagnetic nature of the Ni(II) complexes facilitates NMR characterization, which is often hindered in the presence of paramagnetic metal centers.

Initially, to evaluate the reactivity of the diaminoporphyrin **Ni-2**, acetylacetone was employed as a simple aliphatic *β*-diketone in the condensation reaction (Scheme 1). Unexpectedly, the reaction of **Ni-2** with acetylacetone led to a complex mixture, comprising two major components. Furthermore, the UV-Vis spectrum of this mixture exhibited broad absorption features (Figure S44 in the *Supplementary Materials*). To elucidate the structures of the products, a combination of physicochemical characterization techniques was employed. MALDI-TOF mass spectrometry confirmed the formation of the anticipated diazepine-appended product **Ni-3**, yet also revealed an additional compound with a lower *m/z* value (Figure S45). The detection of this byproduct suggests the occurrence of side reactions, initiated during chromatographic purification, since the MALDI-TOF spectrum of the crude reaction mixture predominantly featured the expected **Ni-3**, along with minor peaks corresponding to dioxochlorin and pyrazine-fused diporphyrin, arising from oxidative degradation of the diaminoporphyrin or parallel condensation pathways.[56–58]

The instability of the diazepine fragment under the reaction conditions is likely attributed to its inherent susceptibility to oxidation at the C(6) position, which can lead to structural rearrangement into a pyrazine core upon exposure to light.[59,60] Similar transformations have been previously reported for diazepine-appended porphyrazines.[61] Interestingly, despite the known tendency of diazepines to undergo such rearrangements, no dimethyl substituted pyrazinoporphyrins were detected in this case. In addition, partial degradation of the diazepine unit to acylated derivatives under acidic conditions has also been documented.[62] Indeed, the formation of **Ni-4** as a N-acylated porphyrin is supported by the presence of a peak at *m/z* 1030.29 in the mass spectrum (Figure S45). This transformation further underscores the reactivity of the diazepine moiety, in which oxidative instability at the C(6) position governs its structural modifications (Scheme 1).

The ^{1}H NMR spectrum of the products mixture revealed distinct signals corresponding to both the symmetric diazepine-appended porphyrin **Ni-3** and the fully desymmetrized molecule **Ni-4** (Figure 1). For **Ni-3**, the *β*-pyrrolic protons appeared as two doublets and one singlet, which correspond to the protons adjacent to the diazepine fragment and the distant pyrrolic positions, respectively. Notably, the *ortho*-protons of the *meso*-aryl substituents exhibited broadening, which is likely caused by restricted rotation of the aryl rings induced by the non-planar configuration of the diazepine moiety. This broadening effect was partially resolved into a broad doublet upon heating to 323 K (Figure S10 in the *Supplementary Materials*).

In contrast, **Ni-4** exhibited a distinct proton resonance at *ca.* 7.0 ppm, consistent with the presence of an acetamide functional group (NHAc). Additionally, a signal in the ^{13}C NMR spectrum ($CDCl_3$) at 166.99 ppm clearly corresponds to the carbonyl carbon of the acetamide moiety. Indeed, in the HMBC, this signal showed correlations with the adjacent aliphatic CH_3 group and the NH proton, further supporting the structural assignment of **Ni-4** (Figure S9).

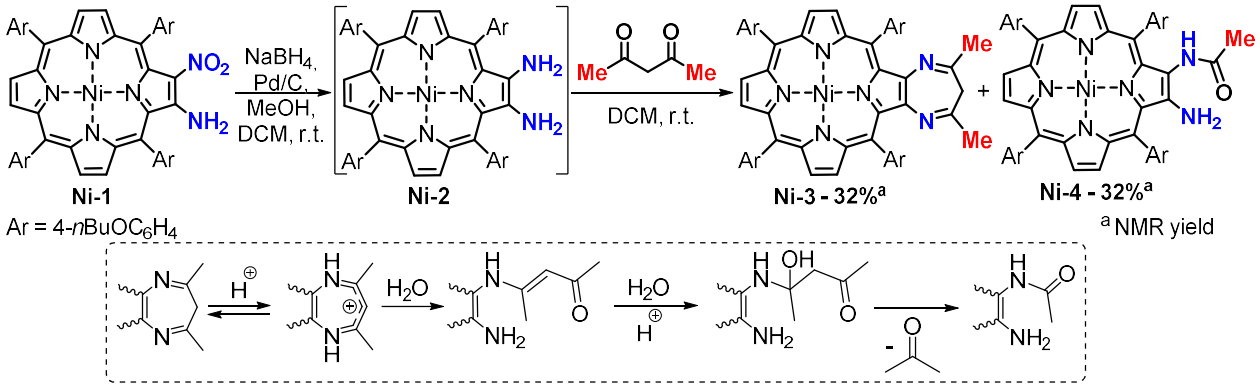

Scheme 1. Condensation of 2,3-diaminoporphyrin **Ni-2** with acetylacetone and presumable path of formation of **Ni-4**.

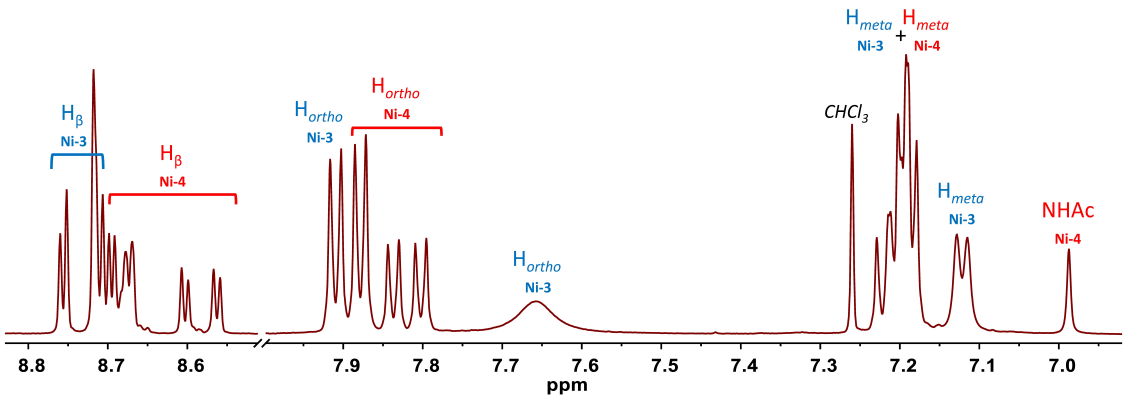

Figure 1. ^{1}H NMR spectrum ($CDCl_3$) of mixture of **Ni-3** and **Ni-4** in 1:1 ratio.

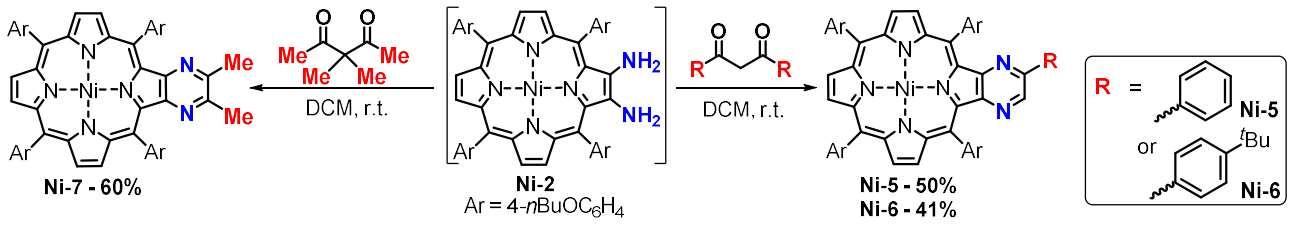

Scheme 2. Condensation **Ni-2** and *β*-diketones with bulky substituents or disubstituted *β*-diketone.

The integral intensities of signals in the ^{1}H NMR spectrum confirmed a 1:1 ratio of **Ni-3** and **Ni-4** in the mixture. Accordingly, both compounds were obtained in 32% yield. These findings suggest that the conditions of the condensation reaction, along with subsequent chromatographic purification, played a critical role in the partial degradation of the diazepine framework.

L-Proline has been reported as an efficient and selective organocatalyst for the synthesis of 1,5-benzodiazepines *via* the condensation of *o*-phenylenediamine with 1,3-dicarbonyl compounds, primarily by activating carbonyl groups, stabilizing intermediates, and promoting cyclization under mild conditions.[44] However, when various amino acid-based catalysts (20 mol%), including *L*-proline, dipicolinic acid, tryptophan, and arginine, were applied to the condensation of **Ni-2** with acetylacetone, the reaction resulted in complex mixtures of inseparable and unidentified products. Among these, compounds **Ni-3** and **Ni-4** were detected based on the molecular ion peaks observed in the MALDI-TOF spectra of the chromatographic fractions.

It was anticipated that replacing the methyl substituents of the β-diketone with bulkier, sterically demanding groups could potentially mitigate the degradation of the diazepine fragment. To test this, condensation reactions of **Ni-2** were carried out with β-diketone derivatives bearing sterically hindered substituents, namely 1,3-diphenylpropane-1,3-dione and 1,3-bis(4-(*tert*-butyl)phenyl)propane-1,3-dione (Scheme 2).

Unexpectedly, the mass spectra unequivocally revealed the formation of a single product in each case, while neither reaction led to the formation of the target diazepine-appended porphyrin or any detectable degradation products. The corresponding ^{1}H NMR spectra confirmed the formation of fully unsymmetric compounds, identified as **Ni-5** or **Ni-6**, each characterized by six distinct doublets in the *β*-proton region (Figure 1, A/B). Furthermore, the ^{1}H NMR spectra displayed a set of signals with integral intensity corresponding to the presence of a single phenyl or *tert*-butylphenyl substituent, along with a singlet significantly shifted downfield, which suggested the formation of mono-substituted pyrazinoporphyrins during the reaction.

The observed upfield shift of the *ortho*-protons of the phenyl group in **Ni-5** and **Ni-6** may be attributed to a possible orthogonal arrangement between the *meso*-aryl substituent and the phenyl fragment of the pyrazine unit, which could lead to magnetic shielding of the corresponding protons. The presence of single peaks of reaction products in the HRMS ESI spectra further corroborated the exclusive formation of **Ni-5** and **Ni-6** (Figure S46/47 in the *Supplementary Materials*). Similar products have previously been reported in studies involving the condensation of *ortho*-diamines with dibenzoylethylenes or heterocyclic *ortho*-diamines with diaroylethylenes.[63–65]

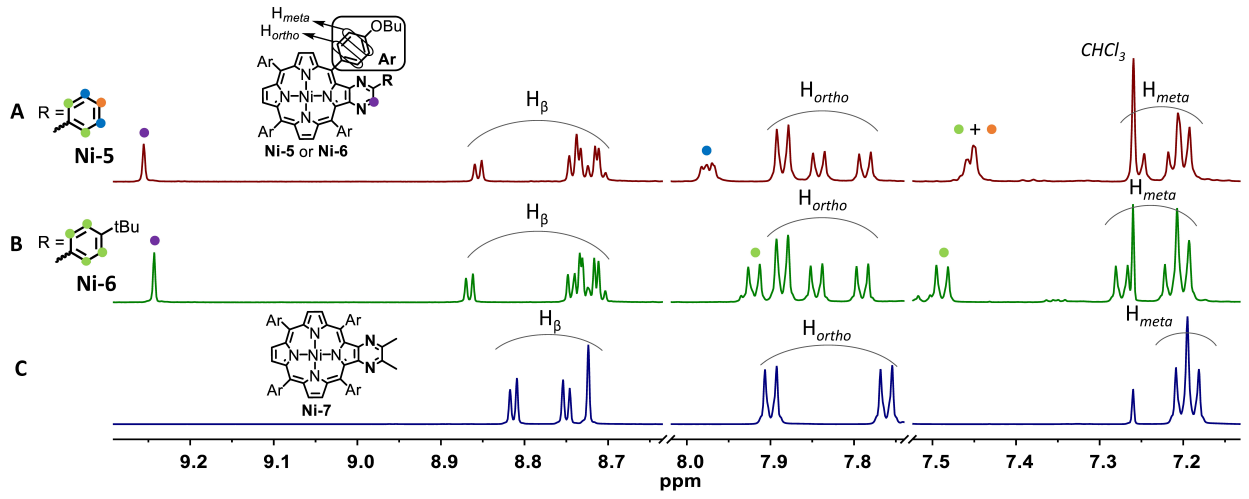

Figure 2. ^{1}H NMR spectrum of **Ni-5 – Ni-7** ($CDCl_3$).

Following these results, an *α,α*-disubstituted *β*-diketone was selected to further investigate the outcome of the reaction. To this end, the condensation of diaminoporphyrin **Ni-2** with dimethylacetylacetone was conducted (Scheme 2). In contrast to the previous reactions, this transformation resulted in a symmetric *β,β'*-appended porphyrin derivative, as confirmed by the ^{1}H NMR spectrum (Figure 2,C). The spectrum displayed two doublets and a singlet corresponding to *β*-pyrrolic protons. Additionally, a singlet in the aliphatic region showed an integral intensity consistent with the presence of two methyl substituents. Based on these observations, the product was identified as the dimethyl substituted pyrazinoporphyrin **Ni-7**. The structure of **Ni-7** was further corroborated by a distinct molecular ion peak in the MALDI-TOF mass spectrum (Figure S48).

The structures of the obtained products **Ni-5 – Ni-7** are not obvious a priori and comprise both symmetric and unsymmetric architectures, giving rise to diverse and non-trivial proton-carbon correlation patterns. Even in the case of symmetrical tetraarylporphyrins the unambiguous interpretation of the NMR data requires considerable efforts,[66,67] while the detailed interpretation of the ^{13}C NMR spectra provides critical insight into the carbon framework. Accordingly, a stepwise strategy was employed for assignment of ^{13}C NMR signals, supported by two-dimensional heteronuclear experiments (Section 1 in the *Supplementary Materials*). The ^{13}C NMR spectra of all compounds can be divided into distinct aromatic and aliphatic carbon regions. Assignments of protonated carbon atoms were established using combination of DEPT-135 and HSQC spectra, whereas quaternary carbons were assigned on the basis of long-range correlations observed in the HMBC spectra (Figure 3).

In the aliphatic region, HSQC correlations allowed reliable identification of the signals corresponding to the butoxy chains, along with the methyl substituents in **Ni-7** and the tert-butyl fragment in **Ni-6** (Figures S19/30/40). In the aromatic region, all *β*-carbons (CH_{β}) of the porphyrin macrocycle were confidently assigned (Figure S18/29/39). In addition, carbons at the *ortho*- and *meta*-positions of the aryl substituents (CH_o and CH_m) were identified based on their correlations with the corresponding aromatic protons. The aromatic carbons of the phenyl substituent (CH_{Ph}) at the *ortho*-, *meta*-positions were assigned for **Ni-5** and **Ni-6**, while the carbon at the *para*-position was additionally identified for **Ni-6**. For both **Ni-5** and **Ni-6**, the protonated carbon of the pyrazine fragment (CH_{Pz}) was also directly observed.

The assignment of these protonated carbons provided a solid basis for the unequivocal linkage of quaternary carbons contiguous to them *via* long-range heteronuclear correlations (Figures S20–21/31–32/42–43). Despite differences in the substituents of the appended fragments across the series, all three compounds **Ni-5 – Ni-7** possess a common tetraarylporphyrin scaffold. Accordingly, their HMBC spectra display characteristic long-range correlation patterns. Specifically, correlations were observed from porphyrin *β*-carbons to the adjacent six C_{α} carbons, as well as from *ortho*- and *meta*-aryl protons to the corresponding ipso aromatic carbons (C_{Ar} and $C_{Ar'}$). In addition, the O-CH_2 protons of the butoxy fragment exhibit long-range correlations to the $C_{Ar'}$ carbons, whose downfield shift are consistent with the negative inductive effect of the oxygen atom. Similarly, the *meso*-carbons of the porphyrin core (C_{meso}) were assigned *via* HMBC correlations originated from the *ortho*-protons of the aryl substituents.

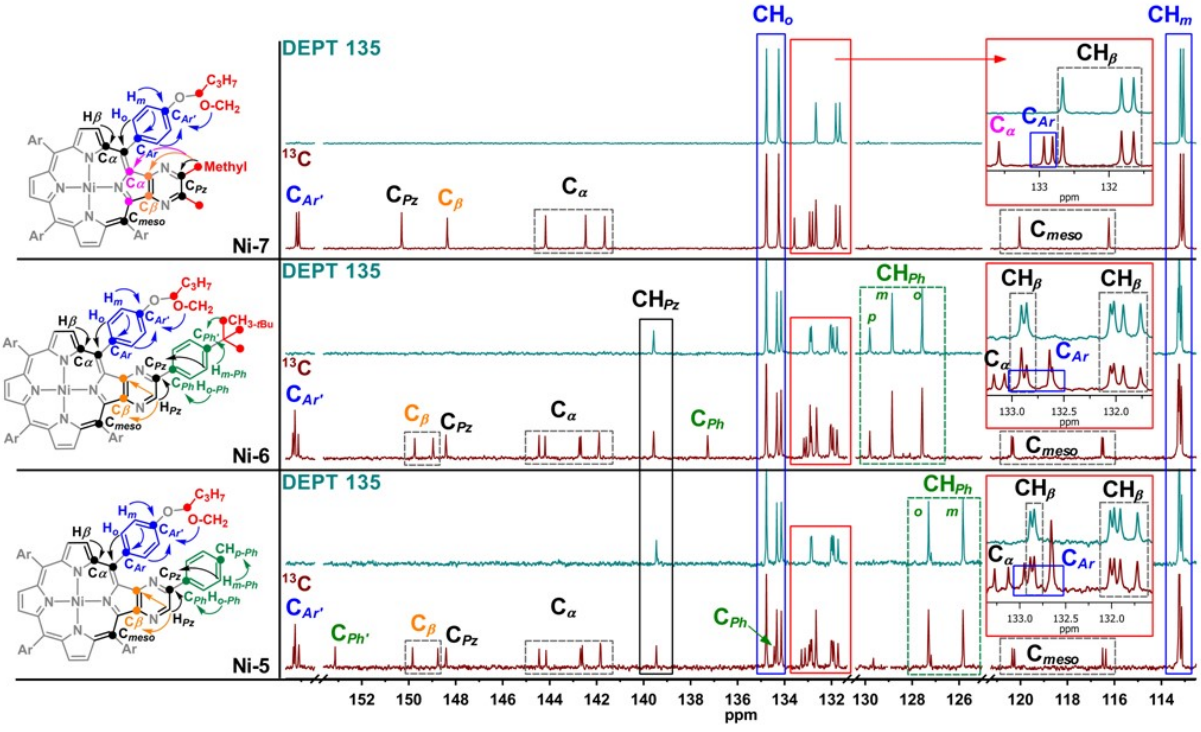

Figure 3. The assignment of the ^{13}C NMR and DEPT-135 spectra ($CDCl_3$) of **Ni-5 – Ni-7**. Arrows indicate long-range heteronuclear correlations observed in the HMBC spectra used for the interpretation of ^{13}C NMR spectra).

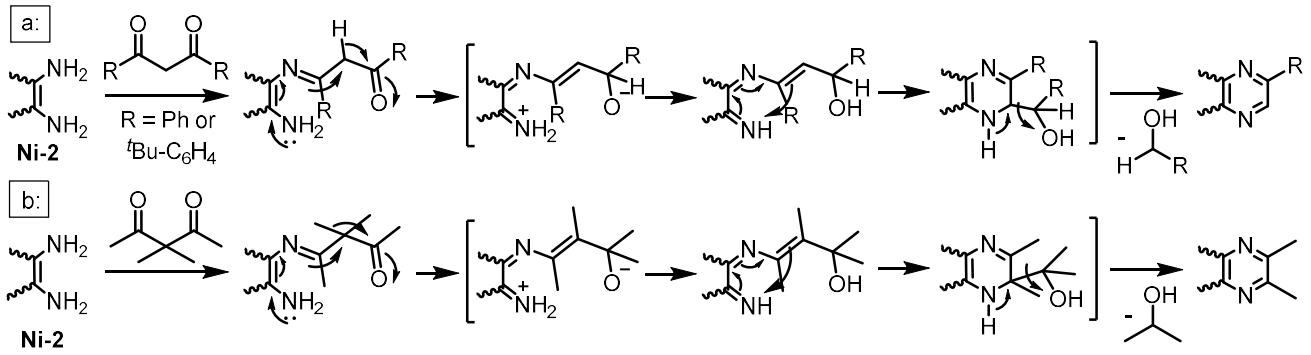

Scheme 1. Possible ways of formation of mono- or di-substituted pyrazinoporphyrins.

Substituents within the appended heterocyclic fragments, as well as the presence of a pyrazine CH unit in **Ni-5 – Ni-6**, allows assignment of the adjacent quaternary carbon centers. For the most symmetric compound in the series **Ni-7**, the HMBC spectrum exhibits correlations from the methyl protons to C_{Pz} and C_{β}, along with weaker correlations through five bonds to the C_{α} carbons near the pyrazine fragment. In the unsymmetric derivatives **Ni-5–Ni-6**, the presence of H_{Pz} enabled assignment of the pyrazine carbons (C_{Pz}) and the neighboring β-carbons. The absence of HMBC correlations to the C_{α} carbons necessitated their assignment by exclusion based on the remaining available resonances. In addition, aromatic protons of the phenyl and *tert*-butylphenyl substituents in **Ni-5** and **Ni-6** exhibit correlations to the corresponding ipso carbons (C_{Ph}). For the *tert*-butyl substituted derivative **Ni-6**, additional HMBC correlations from the methyl groups in ^{t}Bu to the ipso phenyl carbon ($C_{Ph'}$) further confirm the substitution pattern.

Overall, the combination of DEPT-135, HSQC, and HMBC experiments enabled consistent correlation of the carbon signals with the proposed structures for both the unsymmetric **Ni-5 – Ni-6** and symmetric **Ni-7** derivatives. For the mixture of **Ni-3** and **Ni-4**, complete assignment of all carbon signals in ^{13}C NMR was precluded by extensive signal overlap. Nevertheless, characteristic spectral regions corresponding to the key structural motifs were identified, and key HMBC correlations have been identified, enabling reliable structural characterization of both components (Figures S3–4, S7 and S9).

We propose the following mechanism for the formation condensed pyrazinoporphyrins **Ni-5 – Ni-7** through the interaction of diaminoporphyrins with β-diketones (Scheme 3). The reaction is initiated by nucleophilic attack of an amino group in diaminoporphyrin **Ni-2** on the carbonyl carbon of a β-diketone, forming a Schiff-base intermediate and followed by either a 1,2-hydride migration (Scheme 3, pathway a) or a 1,2-methyl migration (Scheme 3, pathway b). A subsequent 6π electrocyclization affords a cyclic intermediate, which completes pyrazine-ring formation through an elimination step. Sterically hindered aryl substituents in the diketone, as well as the use of α,α-disubstituted derivative, influence the relative rates of these migrations and thereby the distribution of mono- *vs* disubstituted products. It testifies the formation of these compounds to be more advantageous from the viewpoint of thermodynamics in comparison with the formation of seven-membered dihydrodiazepine systems.

Table 1 presents the UV-Vis absorption spectra of the obtained pyrazinoporphyrins **Ni-5 – Ni-7**, along with parent tetra(4-butoxyphenyl)porphyrinate nickel(II) **Ni-TBPP**. The absorption bands of all pyrazinoporphyrins exhibit a substantial bathochromic shift relative to **Ni-TBPP**, attributed to effective π-conjugation between the pyrazine fragment and the porphyrin core. Notably, the monosubstituted pyrazinoporphyrins **Ni-5** and **Ni-6** display substantial bathochromic shifts in both the Soret and Q-bands, reaching up to 21 nm, which may be due to steric repulsion between the phenyl substituent in the pyrazine ring and the aryl groups at the *meso*-positions. In contrast, **Ni-7** exhibits a smaller shift *ca.* 12 nm.

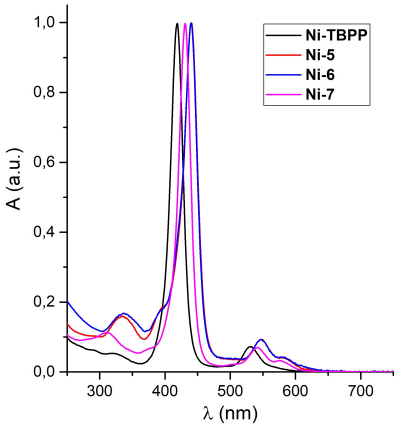

Table 1. UV-Vis data of nickel(II) complexes **Ni-5 – Ni-6** and **Ni-TBPP** in chloroform.

	Soret band [nm] (log ε)	Q_1 band [nm] (log ε)	Q_2 band [nm] (log ε)
Ni-TBPP	419 (5.39)	531 (4.26)	580 (3.33)
Ni-5	440 (5.31)	549 (4.27)	581 (3.91)
Ni-6	440 (5.20)	547 (4.20)	582 (3.88)
Ni-7	431 (5.37)	541 (4.21)	577 (3.88)

Conclusions

This study investigated the synthetic potential of 2,3-diaminoporphyrins as a platform for constructing of heterocycle-appended porphyrin derivatives *via* condensation with various *β*-diketones. It is shown that the nature of the diketone plays a crucial role in determining the reaction path. Condensation with acetylacetone led to the formation of a mixture of two major products, namely, diazepine-appended porphyrin and an acylated byproduct, highlighting both the high reactivity of the substrate and oxidative sensitivity of the diazepine core. In contrast, the use of sterically hindered and *α,α*-disubstituted diketones, aimed at mitigating undesired side reactions, unexpectedly led to the selective formation of stable symmetric or unsymmetric six-membered pyrazine-fused porphyrins. UV-Vis spectra revealed significant bathochromic shifts for pyrazinoporphyrins in both the Soret and Q-bands up to 21 nm, attributed to expanded aromatic system by fusion with the pyrazine fragment.

Acknowledgements. This work was supported by the Ministry of Science and Higher Education of the Russian Federation. The work was performed with the aid of equipment of the Shared Facility Center CKP FMI of the Frumkin Institute of Physical Chemistry and Electrochemistry, Russian Academy of Sciences. The authors are sincerely grateful to P.A. Tarakanov for kindly supplying the *β*-diketone derivatives employed in this work.

References

1. Chahal M.K. *Beilstein J. Org. Chem.* **2024**, *20*, 3085–3112.
2. Silvestri S., Fajardo A. R., Iglesias B. A. *Environ. Chem. Lett.* **2022***, 20,* 731–771.
3. Pereira C.F., Figueira F., Mendes R.F., Rocha J., Hupp J.T., Farha O.K., Simões M.M.Q., Tomé J.P.C., Paz F.A.A. *Inorg. Chem.* 2018, 57, 3855–3864.
4. Polivanovskaia D.A., Abdulaeva I.A., Birin K.P., Gorbunova Y.G., Tsivadze A.Y. *J. Catal.* **2022**, *413*, 342–352.
5. Abdulaeva I.A., Birin K.P., Chassagnon R., Bessmertnykh-Lemeune A. *Catalysts* **2023**, 13, 402.
6. Huang H., Song W., Rieffel J., Lovell J.F. *Front. Phys.* **2015**, *3*, 1–15.
7. Lima E., Reis L.V. *Molecules* **2023**, *28*, 5092.
8. Ethirajan M., Chen Y., Joshi P., Pandey R.K. *Chem. Soc. Rev.* **2011**, *40*, 340–362.
9. Chou J., Kosal M.E., Nalwa H.S., Rakow N.A., Suslick K.S. In: *Porphyrin Handbook, Vol. 6,* **2000**. pp. 43–131.
10. Zhang X., Wasson M.C., Shayan M., Berdichevsky E.K., Ricardo-Noordberg J., Singh Z., Papazyan E.K., Castro A.J., Marino P., Ajoyan Z., Chen Z., Islamoglu T., Howarth A.J., Liu Y., Majewski M.B., Katz M.J., Mondloch J.E., Farha O.K. *Coord. Chem. Rev.* **2021**, *429*, 213615.
11. Li L.-L., Diau E.W.-G. *Chem. Soc. Rev.* **2013**, *42*, 291–304.
12. Moura N.M.M., Faustino M.A.F., Neves M.G.P.M.S. *Molecules* **2020**, *25*, 433.
13. Urbanska K., Farinone M., Pawlicki M. *Met. Tuning Prop. Appl.* **2021**, 1–55.
14. Costa L., Costa J., Tomé A. *Molecules* **2016**, *21*, 320.
15. Abdulaeva I.A., Birin K.P., Bessmertnykh-Lemeune A., Tsivadze A.Y., Gorbunova Y.G. *Coord. Chem. Rev.* **2020**, *407*, 213108.
16. Vallejo M.C.S., Reis M.J.A., Pereira A.M.V.M., Serra V.V., Cavaleiro J.A.S., Moura N.M.M., Neves M.G.P.M.S. *Dyes Pigm.* **2021**, *191*, 109298.
17. Syrbu S.A., Kiselev A.N., Lebedev M.A., Kibireva Y.E. *ChemChemTech* **2025**, *68*(7), 48–56. doi: 10.6060/ivkkt.20256807.7237.
18. Zhdanova K., Vyal'ba F., Bragina N. *Macroheterocycles* **2024**, *17*, 150–179. doi: 10.6060/mhc245875z
19. Ullah F., Ullah S., Khan M.F.A., Mustaqeem M., Paracha R.N., ur Rehman M.F., Kanwal F., ul Hassan S.S., Bungau S. *Molecules* **2022**, *27*, 6631.
20. Amin A., Qadir T., Sharma P.K., Jeelani I., Abe H. *Open Med. Chem. J.* **2022**, *16*, 1–27.
21. Brishty S.R., Hossain M.J., Khandaker M.U., Faruque M.R.I., Osman H., Rahman S.M.A. *Front. Pharmacol.* **2021**, *12*, 762807.
22. Glorius F. In: *N-Heterocyclic Carbenes in Transition Metal Catalysis*, *Vol. 21*, Springer Berlin Heidelberg, **2007**. pp. 1–20.
23. Valdés C., Bayod M. In: *Modern Heterocyclic Chemistry*, *Vol 4,* Wiley, **2011**. pp. 2175–2230.
24. Malki Y., Martinez J., Masurier N. *Med. Res. Rev.* **2021**, *41*, 2247–2315.
25. Leśniewska A., Przybylski P. *Eur. J. Med. Chem.* **2024**, *275*, 116556.
26. Meanwell N.A., Walker M.A. In: *Comprehensive Heterocyclic Chemistry III*, *Vol. 13*, Elsevier, **2008**. pp. 183–235.
27. Donzello M.P., Ercolani C., Stuzhin P.A., Chiesi-Villa A., Rizzoli C. *Eur. J. Inorg. Chem.* **1999**, 2075–2084.
28. Donzello M.P., Dini D., D'Arcangelo G., Ercolani C., Zhan R., Ou Z., Stuzhin P.A., Kadish K.M. *J. Am. Chem. Soc.* **2003**, *125*, 14190–14204.
29. Donzello M.P., Ercolani C., Mannina L., Viola E., Bubnova A., Khelevina O.G., Stuzhin P.A. *Aust. J. Chem.* **2008**, *61*, 262–272.
30. Knyukshto V.N., Kuzmitsky V.A., Borisevich E.A., Volkovich D.I., Bubnova A.S., Stuzhin P.A., Solovyov K.N. *J. Appl. Spectrosc.* **2009**, *76*, 341–351.
31. Tarakanov P.A., Donzello M.P., Koifman O.I., Stuzhin P.A. *Macroheterocycles* **2011**, 4, 177–183.
32. Stuzhin P.A., Tarakanov P., Shiryaeva S., Zimenkova A., Koifman O.I., Viola E., Donzello M.P., Ercolani C. *J. Porphyrins Phthalocyanines* **2012**, *16*, 968–976.
33. Piskorz J., Tykarska E., Gdaniec M., Goslinski T., Mielcarek J. *Inorg. Chem. Commun.* **2012**, *20*, 13–17.
34. Malyasova A.S., Kokareva E.A., Tarakanov P.A., Aleksandriiskii V.V., Khelevina O.G., Koifman O.I. *Russ. J. Org. Chem.* **2013**, 49, 1812–1818.
35. Tarakanov P.A., Simakov A.O., Tolbin A.Y., Balashova I.O., Shestov V.I., Tomilova L.G. *Spectrochim. Acta - Part A Mol. Biomol. Spectrosc.* **2015**, *139*, 464–470.
36. Tarakanov P.A., Simakov A.O., Tarakanova E.N., Chernyak A.V., Klykov V., Stuzhin P.A., Pushkarev V.E. *Macroheterocycles* **2018**, *11*, 312–315.
37. Tarakanov P.A., Tarakanova E.N., Dorovatovskii P.V., Zubavichus Y.V., Khrustalev V.N., Trashin S.A., De Wael K., Neganova M.E., Mischenko D.V., Sessler J.L., Stuzhin P.A., Pushkarev V.E., Tomilova L.G. *Dalton Trans.* **2018**, *47*, 14169–14173.
38. Tarakanov P.A., Simakov A.O., Pushkarev V.E., Konev D.V., Goncharova O.A., Slesarenko N.A., Tarakanova E.N., Nefedov S.E., Stuzhin P.A. *Dalton Trans.* **2023**, 52, 2124–2134.
39. Birin K.P., Poddubnaya A.I., Abdulaeva I.A., Gorbunova Y.G., Tsivadze A.Y. *Dyes Pigm.* **2018**, *156*, 243–249.
40. Abdulaeva I.A., Birin K.P., Polivanovskaia D.A., Gorbunova Y.G., Tsivadze A.Y. *RSC Adv.* **2020**, *10*, 42388–42399.

41. Polivanovskaia D.A., Abdulaeva I.A., Birin K.P., Gorbunova Y.G., Tsivadze A.Y. *ChemPlusChem* **2025**, *90*, e202400469.
42. Shremzer E.S., Polivanovskaia D.A., Birin K.P., Gorbunova Y.G., Tsivadze A.Y. *Dyes Pigm.* **2023**, 210, 110935.
43. Lloyd D., Cleghorn H.P. *Adv. Heterocycl. Chem.* **1974**, *17*, 27–43.
44. Goswami P., Das B. *Synth. Commun.* **2010**, 40, 1685–1693.
45. Kumar G., Tomar V., Kumar P., Nemiwal M. *Chemistry Select* **2023**, *8*, e202303181.
46. Maleki A. *Tetrahedron Lett.* **2013**, *54*, 2055–2059.
47. Michalik D., Jiao H., Langer P. *Magn. Reson. Chem.* **2022**, *60*, 845–856.
48. Liu Y., Chen F., He Y.-M., Li C., Fan Q.-H. *Org. Biomol. Chem.* **2019**, *17*, 5099–5105.
49. Horiguchi K., Yamamoto E., Saito K., Yamanaka M., Akiyama T. *Chem. – A Eur. J.* **2016**, *22*, 8078–8083.
50. Luo Z., Yang J., Yao Z., Yang J., Xu L., Shi Q. *Adv. Synth. Catal.* **2023**, *365*, 3527–3534.
51. Dai-Il J., Tae-wonchoi C., Yun-Young K., In-Shik K., You-Mi P., Yong-Gyun L., Doo-Hee J. *Synth. Commun.* **1999**, *29*, 1941–1951.
52. Bhathiwal A.S., Bendi A., Tiwari A. *J. Mol. Struct.* **2022**, *1258*, 132649.
53. Fahad N.G., Imran N.H., Kadhim Kyhoiesh H.A., Al-Hussainawy M.K. *Results Chem.* **2023**, *6*, 101049.
54. Armarego W.L.F. In: *Purification of Laboratory Chemicals*, Elsevier, **2017**, pp. 95–634.
55. Birin K.P., Gorbunova Y.G., Tsivadze A.Y. *RSC Adv.* **2015**, *5*, 67242–67246.
56. Abdulaeva I.A., Polivanovskaia D.A., Birin K.P., Gorbunova Y.G., Tsivadze A.Y. *Mendeleev Commun.* **2020**, *30*, 162–164.
57. Abdulaeva I.A., Birin K.P., Michalak J., Romieu A., Stern C., Bessmertnykh-Lemeune A., Guilard R., Gorbunova Y.G., Tsivadze A.Y. *New J. Chem.* **2016**, *40*, 5758–5774.
58. Oparina A.D., Shremzer E.S., Polivanovskaia D.A., Birin K.P., Tsivadze A.Y. *J. Photochem. Photobiol. A Chem.* **2025**, 116389.
59. Matsumoto M., Iio A., Yonezawa T. *Bull. Chem. Soc. Jpn.* **1970**, *43*, 281–282.
60. Matsumoto M., Matsumura Y., Iio A., Yonezawa T. *Bull. Chem. Soc. Jpn.* **1970**, *43*, 1496–1500.
61. Tarakanova E.N., Tarakanov P.A., Kumeev R.S., Nefedov S.E., Stuzhin P.A. *J. Porphyrins Phthalocyanines* **2021**, *25*, 1203–1211.
62. Begland R.W., Hartter D.R., Jones F.N., Sam D.J., Sheppard W.A., Webster O.W., Weigert F.J. *J. Org. Chem.* **1974**, *39*, 2341–2350.
63. Bass R.G., Crichton D.D., Meetz H.K., Johnson A.F. *Tetrahedron Lett.* **1975**, *16*, 2073–2076.
64. Chebanov V.A., Desenko S.M., Gurley T.W. In: *Azaheterocycles Based on a,ß-Unsaturated Carbonyls*, Springer, Berlin, Heidelberg, **2008**. pp. 149–180.
65. Wawzonek S. *J. Org. Chem.* **1976**, *41*, 310–313.
66. Birin K.P., Gorbunova Y.G., Tsivadze A.Y. *J. Porphyrins Phthalocyanines* **2011**, *15*, 667–673.
67. Birin K.P., Gorbunova Y.G., Tsivadze A.Y. *Dalton Trans.* **2011**, *40*, 11474–11479.

Received 27.11.2025
Accepted 27.01.2026